Dependence of Simulation of Boreal Summer Tropical Intraseasonal Oscillations on the Simulation of Seasonal Mean

R. S. AJAYAMOHAN*

FRCGC, Japan Agency for Marine–Earth Science and Technology, Yokohama, Japan

B. N. GOSWAMI

Centre for Atmospheric and Oceanic Sciences, Indian Institute of Science, Bangalore, India

(Manuscript received 7 September 2005, in final form 22 May 2006)

ABSTRACT

The link between realism in simulation of the seasonal mean precipitation and summer tropical intraseasonal oscillations and their dependence on cumulus parameterization schemes is investigated using the Florida State University Global Spectral Model (FSUGSM). Forty-member model ensemble simulations of the northern summer season are generated for three different cumulus parameterization schemes [namely, Arakawa–Schubert (Naval Research Laboratory; NRL), Zhang and McFarlane (National Center for Atmospheric Research; NCAR), and Emanuel (Massachusetts Institute of Technology; MIT)]. The MIT scheme simulates the regional pattern of seasonal mean precipitation over the Indian monsoon region well but has large systematic bias in simulating the precipitation over the western Pacific and the Maritime Continent. Although the simulation of details of regional distribution of precipitation over the Indian monsoon region by the NRL and NCAR schemes is not accurate, they simulate the spatial pattern of precipitation over the tropical Indo–Pacific domain closer to observation. The NRL scheme seems to captures the observed northward and eastward propagation of intraseasonal precipitation anomalies realistically. However, the simulations of the NCAR and MIT schemes are dominated by a westward propagating component. The westward propagating mode seen in the model as well as observations is indicated to be an equatorial Rossby wave modified by the northern summer mean flow. An examination of the relationship between simulation of the model climatology and eastward propagating character of monsoon intraseasonal oscillations (ISOs) in a limited sample shows that the scheme that simulates better seasonal mean pattern of rainfall over the tropical Indo–Pacific domain also simulates better intraseasonal variance and more realistic eastward propagation of monsoon ISOs. Among the parameters known to be important for meridional propagation of the summer monsoon ISOs, the meridional gradient of mean humidity in the lower atmosphere seems to be crucial in determining the northward propagation in the equatorial Indian Ocean (between 10°S and 10°N). For better prediction of the seasonal mean Indian monsoon, therefore, the model climatology should have minimum bias not only over the Indian monsoon region but also over the entire Indo–Pacific basin.

1. Introduction

The seasonal-mean Indian summer monsoon [June–September (JJAS)] precipitation is closely related to the annual evolution of the tropical convergence zone (TCZ; Ramage 1971; Shukla 1987; Gadgil 2003) and is characterized by some unique regional features. Two bands of large precipitation, one over the continent and north Bay of Bengal and the other over the Indian Ocean between the equator and 10°S, the narrow maximum along the western Ghat with a rain shadow over the southeastern continent together with the maximum over the head Bay of Bengal, are a few such regional features. The rainfall during the summer season, however, is not uniform and is punctuated by active and break spells that are a manifestation of the monsoon intraseasonal oscillations (ISOs).

* Previous affiliation: Center for Ocean–Atmospheric Prediction Studies, The Florida State University, Tallahassee, Florida.

Corresponding author address: R. S. Ajayamohan, Frontier Research Center for Global Change, JAMSTEC, Yokohama 2360001, Japan.
E-mail: ajayan@jamstec.go.jp

DOI: 10.1175/JAS3844.1

The monsoon ISOs comprise a high-frequency westward propagating mode with a period between 10 and 20 days (Krishnamurti and Bhalme 1976; Chatterjee and Goswami 2004) and northeastward propagating lower-frequency band with period between 25 and 80 days (Yasunari 1979; Sikka and Gadgil 1980; Webster et al. 1998; Goswami and Ajayamohan 2001). Both the 10–20-day oscillation and the 25–80-day oscillation contribute significantly to the total intraseasonal variance in the South Asian monsoon domain (Goswami 2005). The 25–80-day oscillations have a very large zonal scale encompassing both the South Asian and East Asia/western North Pacific monsoon regions. The 10–20-day oscillations have a smaller zonal scale and are regional in character. The lag regression of observed 25–80-day filtered precipitation (Fig. 1) with respect to a reference time series of 25–80-day filtered anomalies averaged over the monsoon trough region shows poleward and eastward propagation of precipitation anomalies. The large-scale character is evident with the southeast to northwest oriented band extending from near the date line to around 50°E and moving northward and eastward. This tilt of the precipitation anomalies results in a quadruple structure of the anomalies at zero lag over the Asian monsoon region (Annamalai and Slingo 2001). Note that the precipitation anomalies associated with the mode have large spatial scale similar to the seasonal mean. Zonal propagation characteristics of dominant ISOs are further illustrated in Fig. 2, where wavenumber–frequency spectra of daily precipitation and 850-hPa zonal wind anomalies are plotted. Strong peaks in the positive wavenumber in both precipitation and zonal winds indicate a convectively coupled eastward propagating mode with period between 25 and 80 days and wavenumbers 2–5. While the eastward propagating 25–80-day ISO mode is dominant in observations, there exists a weaker westward propagating mode as well with roughly same period and wavelength range. The existence of a westward propagating mode with period around 16 days is also evident. The dominant monsoon ISO has a large spatial scale similar to that of the seasonal mean and its interannual variability (Sperber et al. 2000; Goswami and Ajayamohan 2001). This may result in strengthening (weakening) the seasonal mean in its active (break) phases. Hence, the monsoon ISOs have the potential to influence the seasonal mean monsoon and its predictability (Goswami and Ajayamohan 2001; Waliser et al. 2003; Gadgil 2003; Ajayamohan and Goswami 2003). It has been shown that monsoon ISOs modulate synoptic activity over the monsoon trough region and thereby influence the rainfall over this region (Goswami et al. 2003). Recent investigations indicate that interaction between ocean and atmosphere on intraseasonal time scales plays an important role in the scale selection and northward propagation of monsoon ISOs (Sengupta et al. 2001; Fu et al. 2002, 2003). In short, monsoon ISOs influence the seasonal mean monsoon and its interannual variability, on one hand, and modulate the synoptic activity and high rain events over the monsoon trough region on the other. Hence, prediction and realistic simulation of monsoon ISOs assumes great significance.

Although the climate models have improved over the last couple of decades in simulating the global climate in general, almost all climate models still have serious systematic bias in simulating the observed features of the tropical intraseasonal oscillations (Slingo et al. 1996; Gadgil and Sajani 1998; Waliser et al. 2003). In a recent study, Waliser et al. (2003) assessed the intraseasonal variability associated with the Asian summer monsoon for 10 atmospheric general circulation models (AGCMs). They find that many models are lacking in representing the intraseasonal variability in the equatorial Indian Ocean. A double convergence zone about the equator and lack of eastward and northward propagation are some of the major problems identified in simulation of intraseasonal oscillations. Unrealistic ISO activity in a model (either high or low activity compared to observations) can lead to unrealistic simulation of internal interannual variability (IAV) simulated by the model and adversely influence simulation of seasonal mean anomalies. As different models that participated in this study used different parameterization schemes for various physical processes, it is difficult to pinpoint one important physical process that is crucial for realistic simulation of summer ISOs. Slingo et al. (1996) examined simulation of equatorially trapped ISOs in 15 AGCMs and find that models with realistic mean states are more likely to produce realistic intraseasonal oscillations. Maloney and Hartmann (2001) used the National Center for Atmospheric Research (NCAR) Community Climate Model version 3 (CCM3) AGCM to study the sensitivity of tropical intraseasonal variability to changes in convective parameterization. They found that the intraseasonal variability in the model is sensitive to parameterization of convective precipitation evaporation in unsaturated environmental air and unsaturated downdrafts. Their model simulations did not show improvement in intraseasonal variability when boundary-layer relative humidity threshold for initiation of convection is increased.

If one starts with the premise that ISOs are instability of the background mean state, driven unstable by convective feedback, it is not surprising that simulation of ISOs is linked with that of the background mean state (Slingo et al. 1996). It may also be noted that the spatial

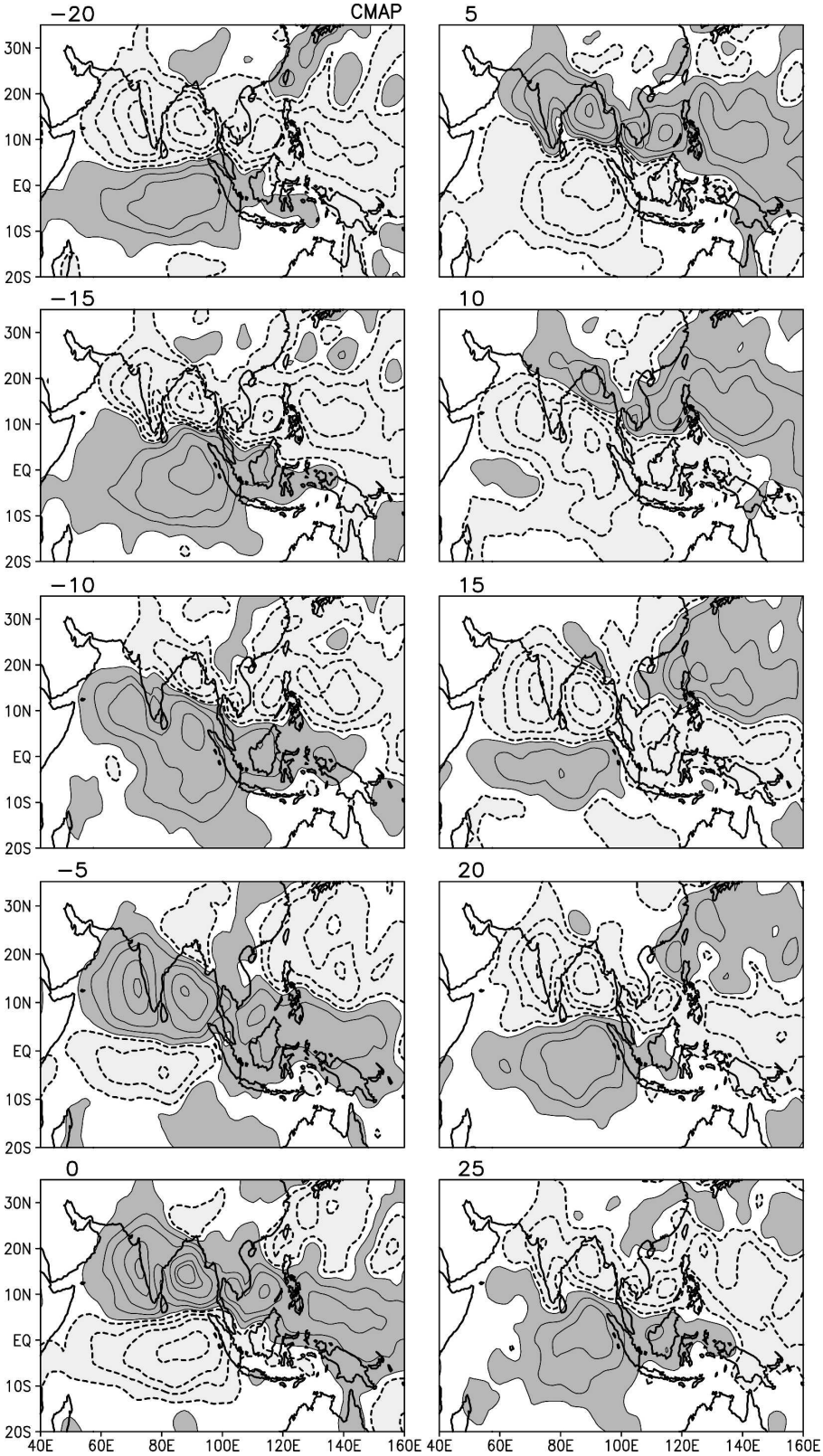

FIG. 1. Evolution of observed precipitation over a cycle of the 25–80-day mode. Regressed 25–80-day filtered anomalies of precipitation (mm day^{-1}) with respect to a reference time series from a lag of 20 days ($t = -20$) to a lead of 25 days ($t = 25$). Solid (dashed) lines indicate positive (negative) contours, with a contour interval of ± 0.5 starting from ± 0.1. Reference time series is constructed by averaging filtered precipitation anomalies over a box in the monsoon trough region (10°–25°N, 70°–95°E) during the summer monsoon season (1 June to 30 September).

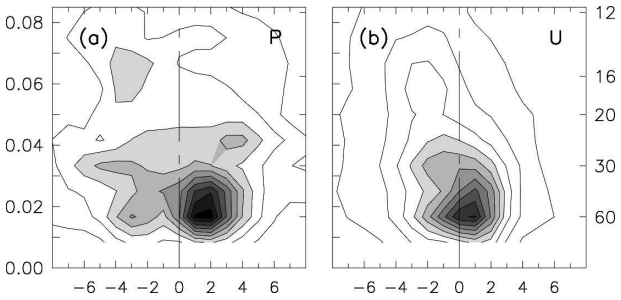

FIG. 2. Wavenumber–frequency spectral power of observed precipitation and 850-hPa zonal winds anomalies averaged over the latitude band 5°–25°N. The *y* axis left ordinate is frequency (in cycles per day, cpd) and right ordinate is period (days), while the *x* axis represents zonal wavenumber. The minimum contour and contour interval is 0.5; contours greater than 2.0 are shaded.

pattern of ISO activity (standard deviation of ISO anomalies) in precipitation is very similar to that of the seasonal mean precipitation (Waliser et al. 2003). Since simulation of the mean state by a climate model depends, among other things, on the cumulus parameterization scheme used by the model, the ability of the model to simulate observed ISO characteristics correctly may also depend on the cumulus parameterization scheme used by the model. The objective of the present study is to investigate the connection between simulation of summer monsoon ISOs, the seasonal mean simulation, and cumulus parameterization schemes. Not many studies have addressed this question in the context of simulation of monsoon intraseasonal variability. A related question is whether realistic simulation of the background mean state over the Indian monsoon region is sufficient for realistic simulation of the ISOs. Does systematic bias in simulating the seasonal mean over a region such as the tropical Pacific have a role to play in simulating the observed characteristics of Indian monsoon ISOs? Another objective of the present study is to address this question.

In the present study we investigate the ability of the recently upgraded FSUGSM (Cocke 1998; LaRow and Krishnamurti 1998; Cocke and LaRow 2000) in simulating the propagation characteristics of monsoon ISOs using three different convective parameterization schemes. We proceed by analyzing the major characteristic of monsoon ISOs; namely, northward and eastward propagation of the precipitation anomalies using three different convection schemes. In this context, we will also examine how the simulation of ISOs is related to the simulation of the seasonal mean. Section 2 gives a brief description of the model, design of the numerical experiments, and the datasets used for the study. Section 3 discusses the model climatology using three different cumulus schemes. Section 4 considers the description on the model simulation of monsoon intraseasonal variability and its propagation characteristics. The probable reasons for the model bias in simulating the observed characteristics of monsoon ISOs and the nature of the westward propagation seen in model simulations is discussed in section 5. Dependence of the seasonal mean in simulating the intraseasonal variability is examined in section 6. Main conclusions of this work are summarized in section 7.

2. Experimental framework and data sources

The FSUGSM has a horizontal resolution of T63 (~1.86°) with 17 unevenly spaced σ levels. Brief description of the model is listed in LaRow and Krishnamurti (1998). The physical parameterization includes fourth-order horizontal diffusion (Kanamitsu et al. 1983), shallow convection (Tiedke 1984), and large-scale condensation (Kanamitsu 1975). Longwave and shortwave radiative fluxes are based on a band model (Harshvardhan and Corsetti 1984; Lacis and Hansen 1974), the surface energy balance is coupled to similarity theory (Krishnamurti et al. 1991) with surface fluxes calculated via similarity theory (Businger et al. 1971). Parameterization of the low, middle, and high clouds is based on threshold relative humidity values. Vertical turbulent transport for heat, momentum, and moisture within the atmosphere are parameterized based on exchange coefficients that are functions of the Richardson number (Louis 1981). Details of the model's physical parameterizations can be found in Krishnamurti et al. (1991).

The original version of the FSUGSM had a modified Kuo-type cumulus scheme (Krishnamurti et al. 1983). In the present study, we compare the performance of the FSUGSM at intraseasonal time scales by replacing the original cumulus convection scheme with three different convective parameterization schemes, summarized in Table 1. They are 1) Naval Research Laboratory/Arakawa–Schubert (NRL/AS; Rosmond 1992); 2) (NCAR/ZM; Zhang and McFarlane 1995); 3) Massachusetts Institute of Technology (MIT; Emanuel and Zivkovic-Rothman 1999). The AS scheme (Hogan and Rosmond 1991; Rosmond 1992) adjusts a model-predicted atmospheric thermodynamic state toward some reference atmosphere. This adjustment must reduce conditional instability in the model atmosphere. Adjustment is initiated when the critical value of cloud work function (a measure of buoyancy of lower tropospheric parcels) for a particular cloud type is exceeded. Cloud types are distinguished by differing entrainment parameters. The Zhang and McFarlane (1995) scheme

TABLE 1. Comparison of the three different cumulus convective parameterization schemes.

Scheme	Reference	Description
NRL	Hogan and Rosmond (1991)	Mass flux based on a quasi-equilibrium assumption of cloud work function
NCAR	Zhang and McFarlane (1995)	Mass flux scheme with saturated downdrafts
MIT	Emanuel and Zivkovic-Rothman (1999)	Predictive equation for mass flux; cloud microphysics included

is based on a plume ensemble approach in which it is assumed that an ensemble of convective-scale updrafts and downdrafts exist when the atmosphere is conditionally unstable in the lower troposphere. The updraft plumes originate in the planetary boundary layer and can penetrate to the upper troposphere to their neutral buoyancy levels. Convection occurs only when there is convective available potential energy, which is subsequently removed by convection using a specified adjustment time scale. Simple assumptions about convective cloud structure are used to determine the mass flux and the thermodynamic properties in the updraft and downdraft ensembles. The cumulus parameterization, developed by Emanuel and Zivkovic-Rothman (1999), is a revision of the parameterization proposed by Emanuel (1991). At the heart of the scheme is the representation of moist convective transport within clouds (subcloud-scale drafts) using a buoyancy sorting technique that determines the level of ascending or descending air parcels by finding the level where the liquid water potential temperature of the parcels equals that of the environment. In contrast to the AS scheme, which diagnostically determines the upward mass flux based on a quasi-equilibrium assumption of the cloud work function, the Emanuel scheme has a predictive equation for mass flux with entrainment and detrainment rate terms determined by the vertical buoyancy gradients. Like the AS scheme, this formulation allows an adjustment to quasi equilibrium, but this adjustment is conditional on the local situation and does not require any assumptions about how far the cloud work function can relax toward its climatological value.

Observed pentad and monthly precipitation datasets based on Climate Prediction Center Merged Analysis of Precipitation (CMAP; Xie and Arkin 1997) for the period 1979–2001 and daily precipitation dataset from Global Precipitation Climatology Project (GPCP; Huffman et al. 2001) for the period 1997–2003 are used for validation of simulated precipitation. The CMAP precipitation dataset is used for calculating climatology and lag regression plots as it has a longer record of data. Since the CMAP does not have a daily record of precipitation data, the GPCP daily precipitation dataset is used for the calculation of wavenumber–frequency spectra and intraseasonal variance. The National Centers for Environmental Prediction (NCEP)/NCAR daily and monthly reanalysis products (Kalnay et al. 1996) were used for validation of the circulation fields.

3. Model climatology

In an effort to construct an optimum model for better simulation of the intraseasonal variability of the Indian monsoon, we examined how the Indian summer monsoon is simulated by the model with these different cumulus schemes. For this purpose, five-member ensemble simulations for five months (May–September) with different initial conditions were carried out for eight years (1987–94). Initial conditions starting 1 May are taken from corresponding 1200 UTC European Centre for Medium-Range Weather Forecasts (ECMWF) analysis and differ from each other by one day. Thus, we have a sample of 40 ensembles for each convection scheme. Model runs were carried out with prescribed weekly mean SST data derived from Reynolds and Smith (1994). Northern summer (June–September; JJAS) precipitation climatology calculated from the ensemble mean of these 40 samples for each convection scheme is compared with the observed (CMAP) climatology (Fig. 3). All cumulus schemes have difficulty of one type or other in simulating the summer mean precipitation over the Indian monsoon domain. Both NRL and NCAR schemes fail to capture the correct geographical location of the secondary zone of maximum precipitation over the south equatorial Indian Ocean (IO) resulting in a westward-shifted peak with higher amplitude. The MIT scheme simulates the south IO precipitation band southward of the observed location while simulating a zone of no precipitation over the equatorial IO. NRL and NCAR schemes simulate the precipitation over the monsoon trough and Bay of Bengal in a realistic manner. However, the rain-shadow region over the southern tip of the Indian continent is not captured except by the MIT scheme. The major drawback of MIT scheme is poor simulation of the west Pacific and eastern IO rainfall. The magnitude of simulated precipitation is higher than the observed in both NRL and NCAR schemes at almost all locations. An area of high rainfall simulated over southern Arabia by all the three schemes is not seen in observations. The South Pacific convergence zone (SPCZ) simulated by

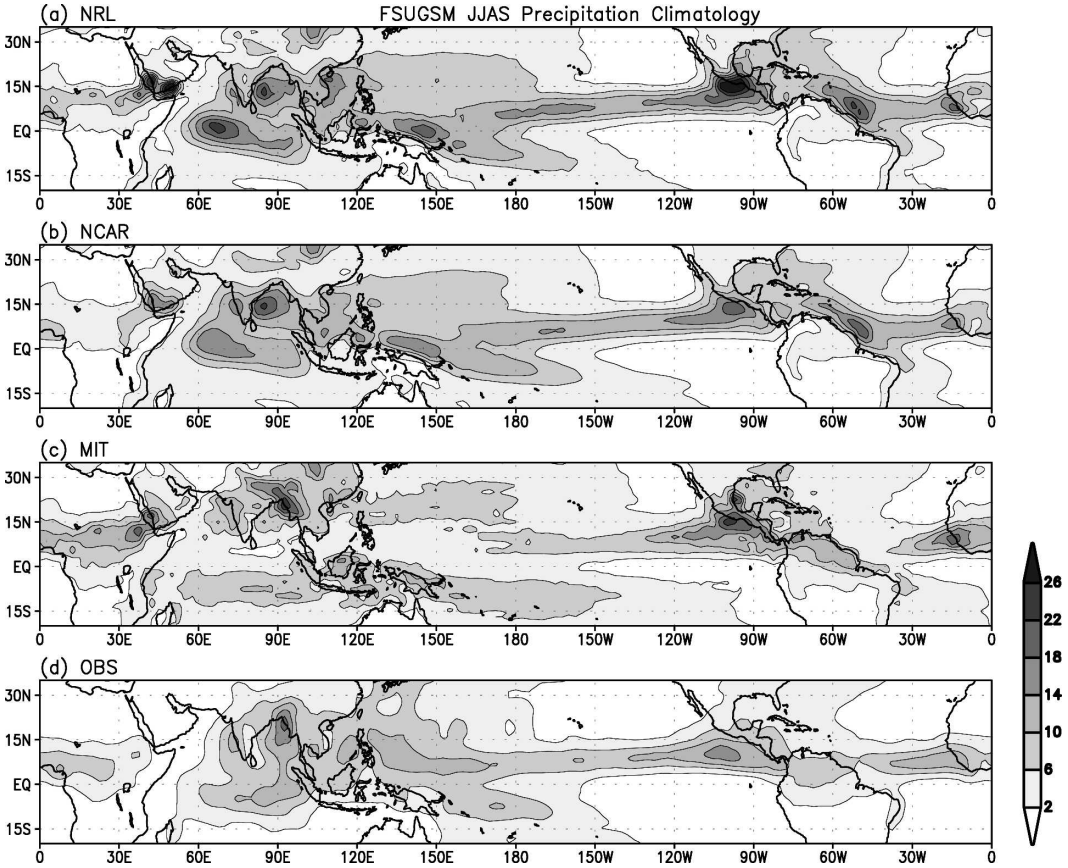

FIG. 3. Ensemble mean JJAS seasonal mean precipitation (mm day^{-1}) simulated by the FSUGSM using different convection schemes.

the MIT scheme is southward of its observed mean position resulting in erroneous precipitation over Indonesia and northern Australia. However, the MIT scheme seems to have good skill in simulating regional distribution of rainfall over the Indian monsoon region. Spatial correlation between the simulated precipitation climatology versus observed climatology in three different domains is summarized in Table 2. The NRL scheme shows a spatial correlation of 0.7 in Indo–Pacific and Indo–west Pacific domains. The NCAR scheme also fares reasonably well in this domain. However, the MIT scheme shows poor skill in simulating the mean precipitation over the Indo–Pacific and Indo–west Pacific domains while showing good skill over the Indian monsoon region.

4. Intercomparison of simulated intraseasonal variability

In this section, we investigate the fidelity of the FSUGSM in simulating observed characteristics of northern summer monsoon intraseasonal oscillations. For this purpose, we have constructed daily anomalies of some fields (precipitation and zonal and meridional winds at 850 and 200 hPa) by removing the annual mean and sum of annual and semiannual harmonics from the daily values. To study the spatial characteristics of the monsoon intraseasonal oscillations, the anomalies for the period 1 June to 30 September from the 40-member ensemble for each cumulus scheme are bandpass filtered using a Lanczos filter (Duchon 1979) to retain periodicities between 25 and 80 days and are referred to as filtered anomalies hereafter.

Figure 4 shows variance of daily filtered anomalies of

TABLE 2. Spatial correlation between model simulated seasonal mean precipitation and observed precipitation for different convection schemes.

Scheme	20°S–30°N, 50°E–120°W	20°S–30°N, 50°–150°E	10°–25°N, 50°–100°E
NRL	0.78	0.70	0.65
NCAR	0.72	0.61	0.50
MIT	0.48	0.38	0.69

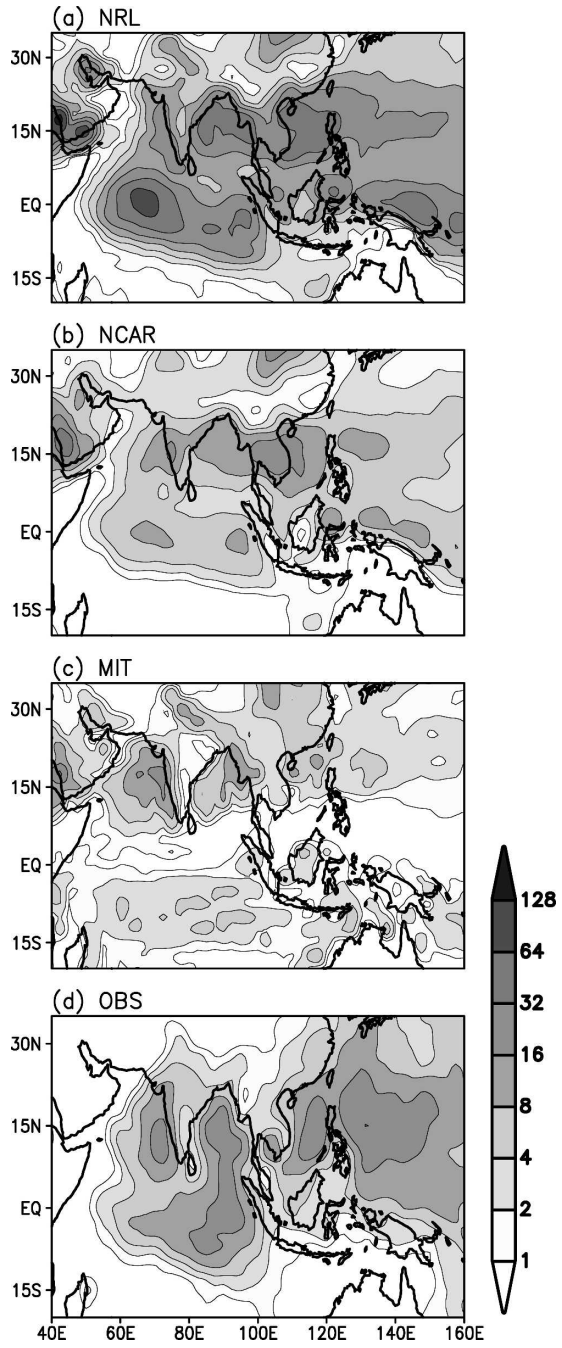

FIG. 4. JJAS seasonal mean variance of filtered precipitation anomalies ($mm^2\ day^{-2}$) simulated by the model for different convection schemes.

simulated precipitation between 1 June and 30 September for the three convective parameterization schemes and compares with a similar plot from observations (CMAP). In observations, as well as in all the three cumulus schemes, the spatial pattern of daily variance bears close similarity with the climatological seasonal mean precipitation (see Fig. 3). Some of the systematic biases of the different schemes in simulating the seasonal mean are also seen in simulating the variance. The magnitude of precipitation variance in the NRL scheme is much higher compared to the observations all over the Indo–west Pacific domain. All three schemes seem to have difficulty in simulating intraseasonal variance over the oceanic TCZ. While the center of ISO activity over the south equatorial precipitation band seems to be shifted westward from the observed position in the NRL and NCAR schemes; it is shifted slightly southward from the mean position in the MIT scheme. The amplitude of oceanic TCZ simulated by the FSUGSM using the NCAR and MIT schemes is weaker compared to observations. The MIT scheme shows a zone of zero precipitation variance over the equator. Consistent with the simulated climatology, the MIT scheme also shows poor simulation of ISO variance over the western Pacific. Erroneous peak of precipitation variance over Arabia seems to occur in all three cumulus schemes. In summary, the NRL scheme fairs better among the three schemes, as far as simulation of the spatial pattern of intraseasonal variance over the Indo–west Pacific domain is concerned, although the amplitude is larger than observed.

To understand the propagation characteristics of monsoon ISOs, filtered precipitation anomalies are regressed with respect to a reference time series and are plotted at different lags. A reference time series is constructed by averaging filtered precipitation anomalies over a box in the monsoon trough region (10°–25°N, 70°–95°E) during the summer monsoon season (1 June to 30 September). The lag-regression plot of filtered anomalies simulated by the NRL scheme (Fig. 5) shows northward and eastward propagation of the band of precipitation anomalies from about 5°S, similar to observations (Fig. 1). The southeast to northwest tilt of the precipitation anomalies at zero lag is also similar to that in observations. Anomalies simulated by the NCAR scheme seem to be more zonal and do not have the observed tilt. They start from about 10°N (Fig. 6, lag = −20) but, instead of propagating northward and eastward, the band propagates northward and westward. This bias is even more striking for the ISO simulated by the MIT scheme (Fig. 7). Instead of orienting from southeast to northwest, the precipitation band is oriented from southwest to northeast and propagates northward and westward. Thus, the fundamental characteristics of the ISOs simulated by the NCAR and MIT schemes are quite different from that observed.

Northward propagation characteristics of model simulated precipitation anomalies are summarized in Figs. 8a–c in which we plot regressed precipitation averaged over 70°–95°E as a function of latitude. The

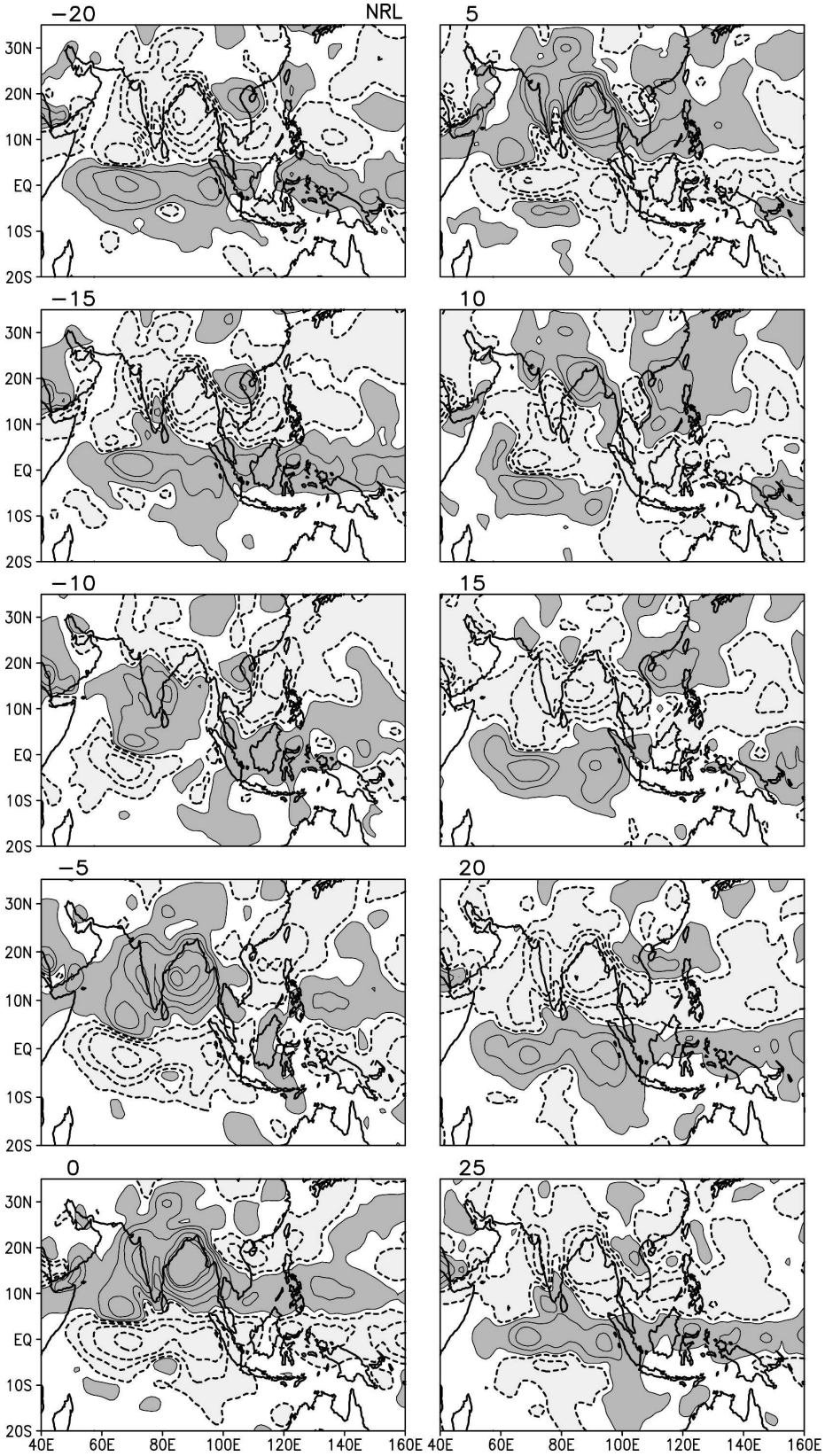

FIG. 5. As in Fig. 1 but using model simulated precipitation with the NRL convection scheme.

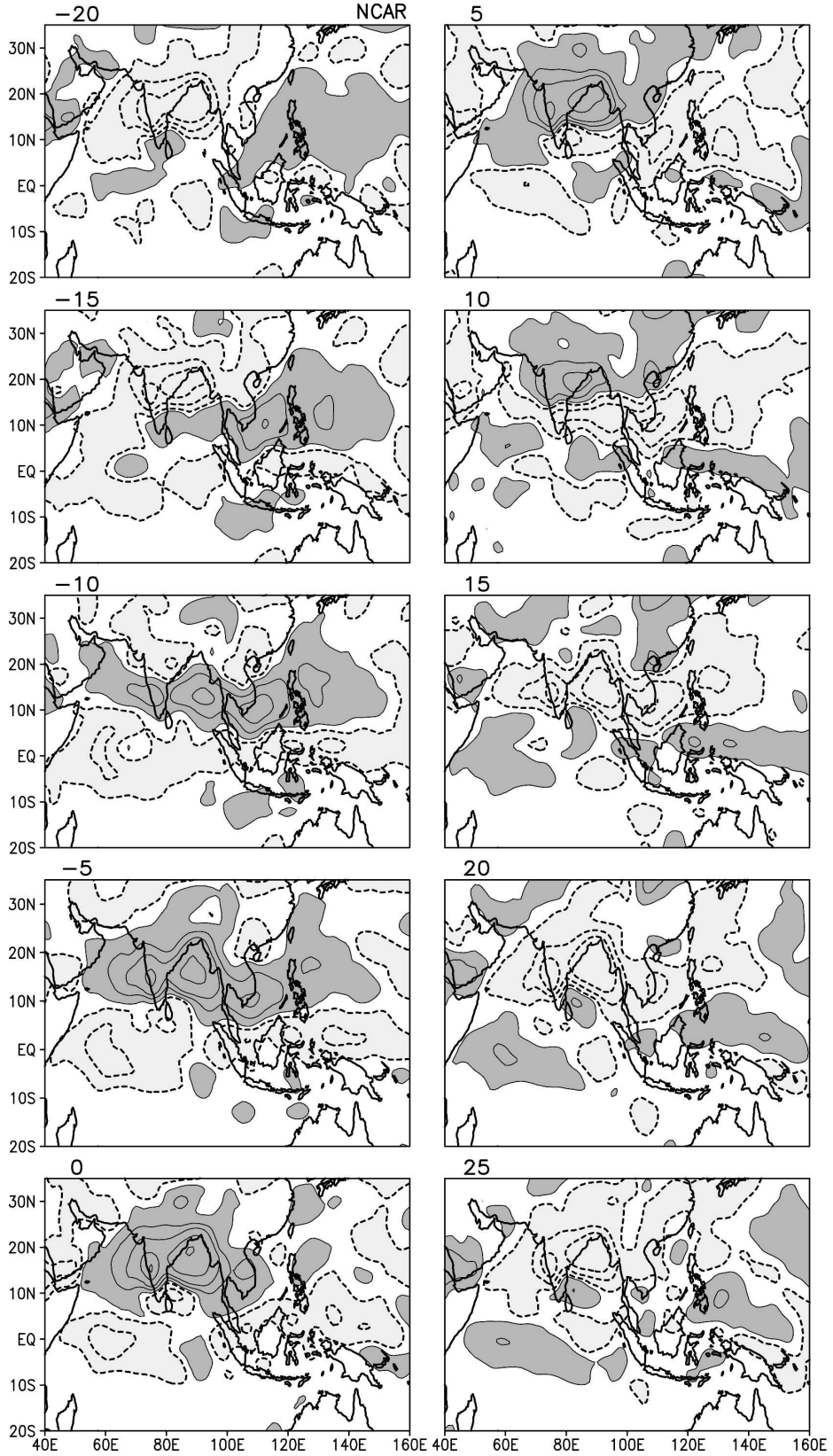

FIG. 6. As in Fig. 1 but with the NCAR convection scheme.

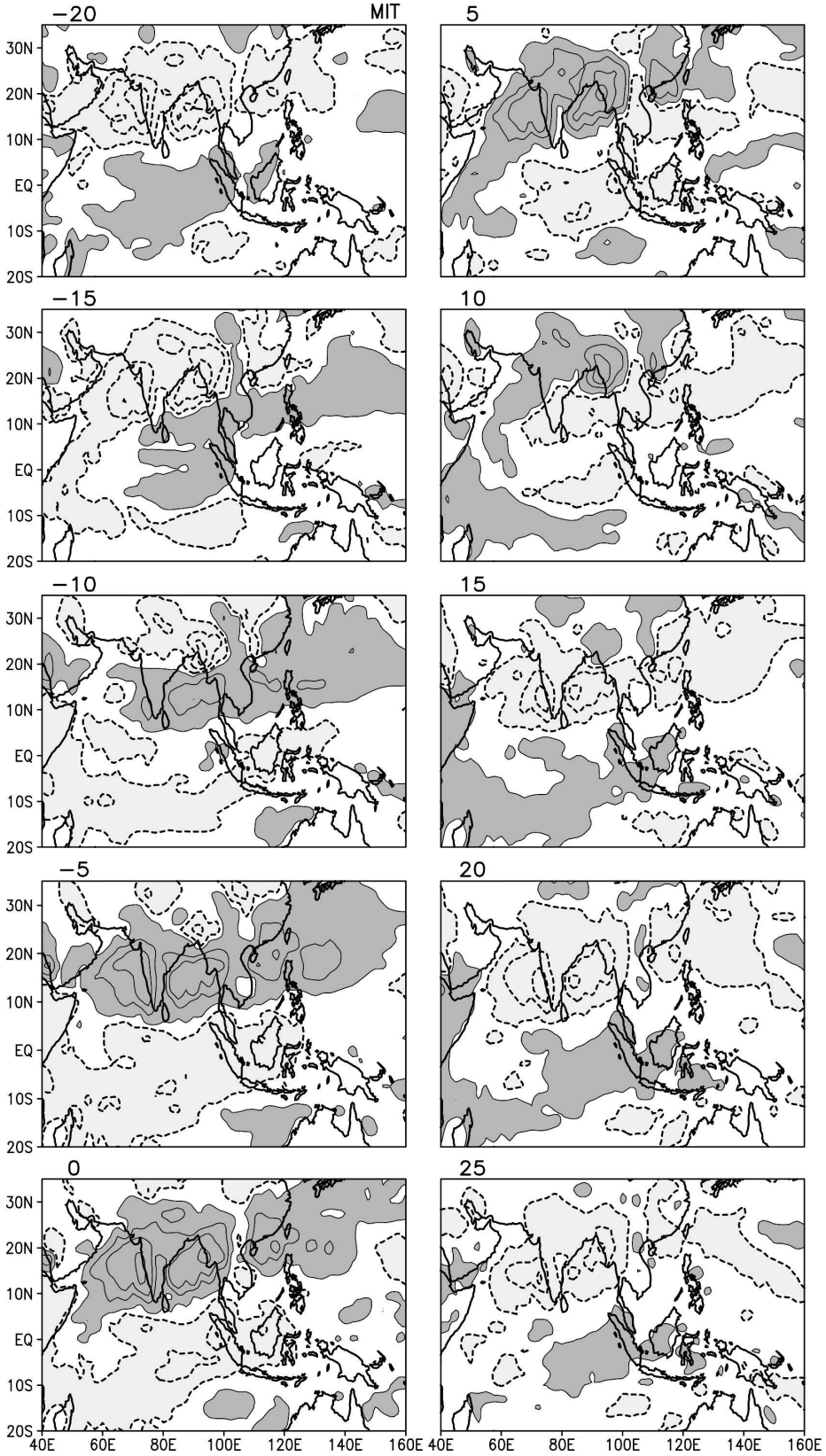

FIG. 7. As in Fig. 1 but with the MIT convection scheme.

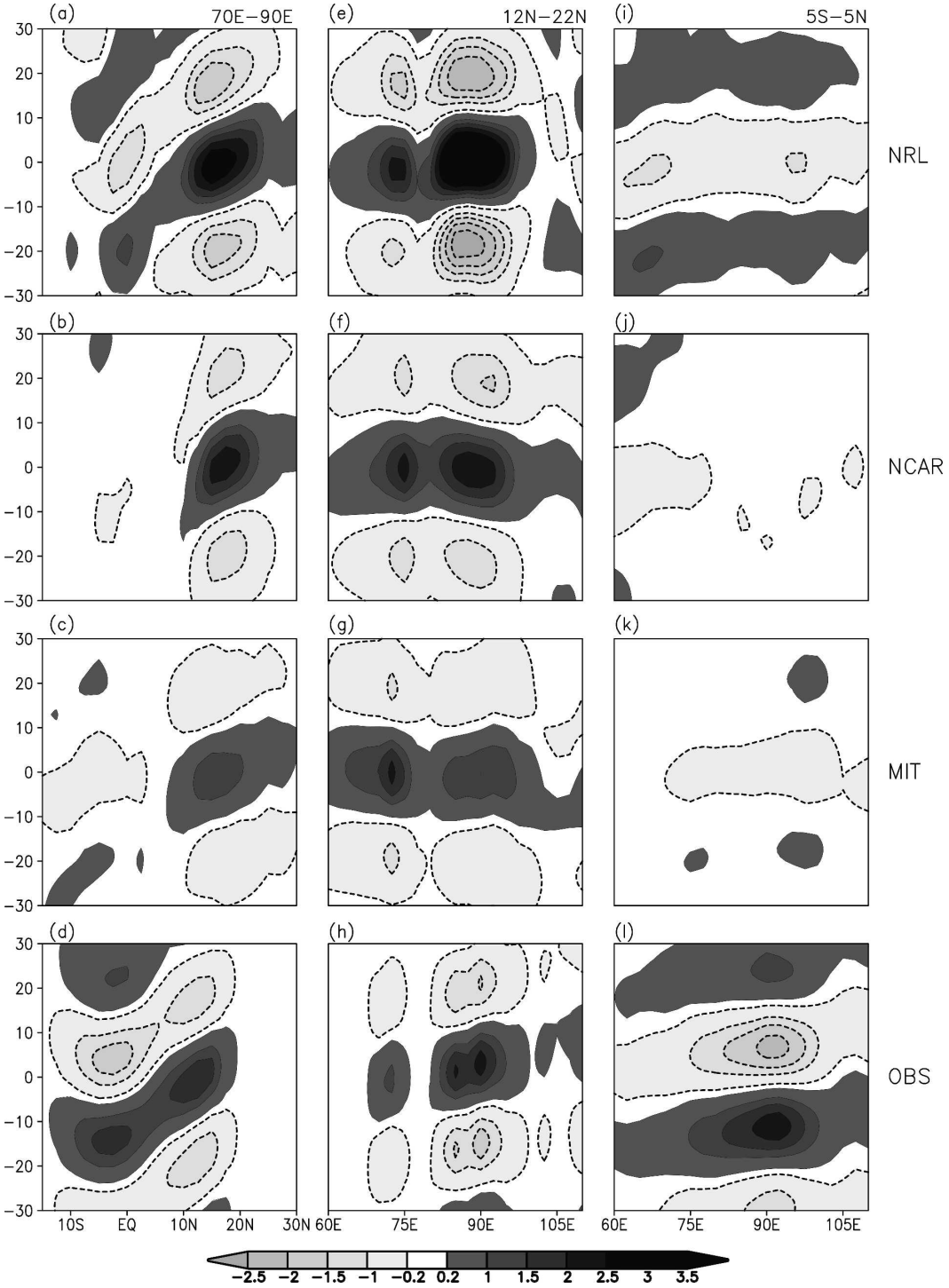

FIG. 8. Regressed 25–80-day filtered anomalies of precipitation (mm day^{-1}) with respect to a reference time series. Contour interval is 0.5 starting from 0.5 mm day^{-1}. (a), (b), (c), (d) Regressed anomalies averaged over 70°–90°E plotted as a function of latitude and time lag for different cumulus schemes compared with observations. (e), (f), (g), (h) Regressed anomalies averaged over 12°–22°N plotted as a function of longitude and time lag for different cumulus schemes compared with observations; (i), (j), (k), (l) same as (e), (f), (g), (h) but for anomalies averaged over 5°S–5°N.

NRL scheme simulates the observed northward propagation characteristics of monsoon ISOs realistically. However, the NCAR and MIT schemes, in general, exhibit weak northward propagation that is confined north of 10°N. Similarly, to examine the east–west propagation characteristics of monsoon ISOs simulated by the model, regressed filtered anomalies are averaged over two domains, one over the continent (12°–22°N) and the other over the equatorial region (5°S–5°N), and plotted as a function of longitude. Observations show an eastward propagating signal over the monsoon trough region (Fig. 8h). It may be noted that both the NCAR and MIT schemes (Figs. 8f,g) indicate westward propagation over the Indian continental region, while only the NRL scheme exhibits reasonable eastward propagation when compared with observations. Over the equatorial domain too, the NRL scheme shows an eastward propagating signal. Both the NCAR and MIT schemes show insignificant anomalies in the equatorial domain.

A wavenumber–frequency spectral technique (Wheeler and Kiladis 1999; Wheeler et al. 2000) is employed to study the eastward and westward propagation characteristics of monsoon ISOs seen in the model simulations. However, decomposing the data into symmetric and antisymmetric components about the equator, as done by Wheeler and Kiladis (1999) and Wheeler et al. (2000), is not suitable for the northern summer ISOs as the maximum amplitude for them is located well north of the equator. Therefore, wavenumber–frequency spectra are calculated from daily anomalies (without decomposing into symmetric and antisymmetric components) by averaging between 5° and 25°N. Wavenumber–frequency spectra calculated from the model-simulated precipitation and 850-hPa zonal wind anomalies for the three different cumulus schemes are shown in Fig. 9. Existence of similar peaks in both the fields (P and U_{850}) indicates that the system is convectively coupled. In general, the FSUGSM has a tendency to simulate a larger westward propagating ISO signal both for precipitation and U_{850}. However, the NCAR and MIT schemes simulate a much weaker eastward propagating ISO signal, allowing the westward propagating ISO signal to dominate. In contrast, the amplitude of the eastward propagating ISO signal simulated by the NRL scheme is comparable in strength to that of the westward propagating ISO signal, resulting in more realistic eastward propagation of the total signal similar to observations (see Fig. 2).

5. Nature of the westward propagating mode

It may be noted that a westward propagating 25–80-day mode with wavenumbers between (−2) and (−5) exists even in observations (Fig. 2a). However, the power of this mode is much weaker than the corresponding eastward propagating mode in observations. From the discussion in the previous section, it is evident that models ability to simulate the observed space–time characteristics of the summer ISOs depend on its fidelity in simulating the eastward propagating component of the ISO relative to the amplitude of the simulated westward propagating component. To study the characteristics of the westward propagating signal, evident in the model simulations, we have used a box-type filter to extract the westward signal in the wavenumber–frequency domain [(−)2 to (−)5 in the wavenumber and 25–80 days in periodicity]. Figure 10 shows the variance of the wavenumber–frequency filtered westward propagating mode seen in the model simulations for all three cumulus schemes compared with a similar plot from observed precipitation. Variance of the westward propagating mode in observed precipitation shows two peaks over the west Pacific, one at about 15°N and another at around 30°N (Fig. 10d). There is also one peak in the eastern Pacific around 10°N and another peak is seen over the equatorial Indian Ocean, almost at the same location of the oceanic tropical convergence zone. The NRL scheme shows high variance over the western Pacific around 15°N, over the eastern Pacific around 10°N, and over the equatorial Indian Ocean (Fig. 10a). However, the NRL scheme fails to simulate the maximum in the western Pacific at about 30°N. The NCAR scheme does not simulate high variance over the Indian Ocean. The peak of variance is shifted toward the Indian continent in the MIT scheme. Consistent with Fig. 9, the variance of the westward propagating mode simulated by the NCAR and MIT schemes is weaker than observed, while that by the NRL scheme is stronger than observed. The spatial pattern of simulated variance by the NRL scheme has a better correspondence with that of the observed compared to those simulated by the NCAR and MIT schemes.

The nature of a westward propagating wave seen in model simulations is further illustrated in Fig. 11, where we show the zero-lag regression plot of 850-hPa wavenumber–frequency filtered winds and vorticity. Regression is calculated with respect to a reference time series of filtered zonal winds at 850 hPa averaged over a box in the west Pacific (13°–15°N, 120°–130°E). This box is selected as the filtered variance at this location is high. All three schemes show similar pattern with each circulation cell moving westward. The observed mode (Fig. 11d) seems to have a wavelength at about 100° longitude (or about 10 000 km). All three schemes simulate the westward propagating mode with roughly

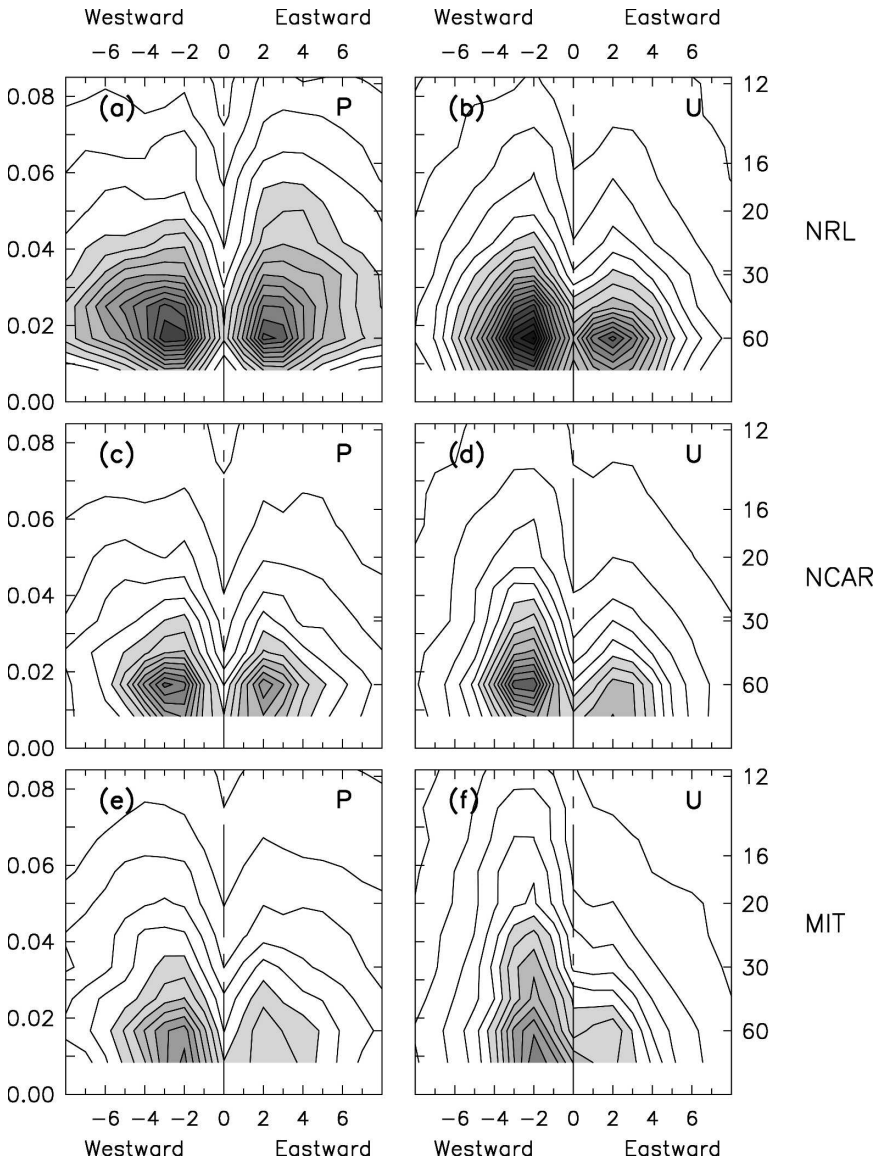

FIG. 9. Wavenumber–frequency spectral power of model simulated precipitation and 850-hPa zonal winds anomalies for the three different cumulus schemes averaged over the latitude band 5°–25°N. The *y* axis left ordinate is frequency (cpd) and right ordinate is period (days), while the *x* axis represents zonal wavenumber. The minimum contour and contour interval is 0.25; contours greater than 1.5 are shaded. (a), (b) Spectral power of precipitation and U_{850} respectively, when NRL scheme is used; (c), (d) for the NCAR scheme and (e), (f) for the MIT scheme. Spectral power of the NRL scheme is divided by an arbitrary number 4 to use the same contour levels for all plots.

the correct wavenumber, consistent with the space–time spectra plot. The mode is a little stronger than observed in the NRL scheme, while it is weaker than observed in the MIT scheme. Thus, it appears that the westward propagating mode is a Rossby wave with a period of about 50 days and wavelength of about 10 000 km. The meridional structure, however, does not confirm to a pure equatorial Rossby wave. It is known that shear of the mean background flow can introduce significant asymmetry to the structure of equatorial waves (Wang and Xie 1996; Xie and Wang 1996; Chatterjee and Goswami 2004). The northern summer tropical quasi-biweekly mode has been recently shown to be an $n = 1$ equatorial Rossby wave of wavelength about 6000 km translated to about 5° north of the equator by the background mean shear by Chatterjee and Gos-

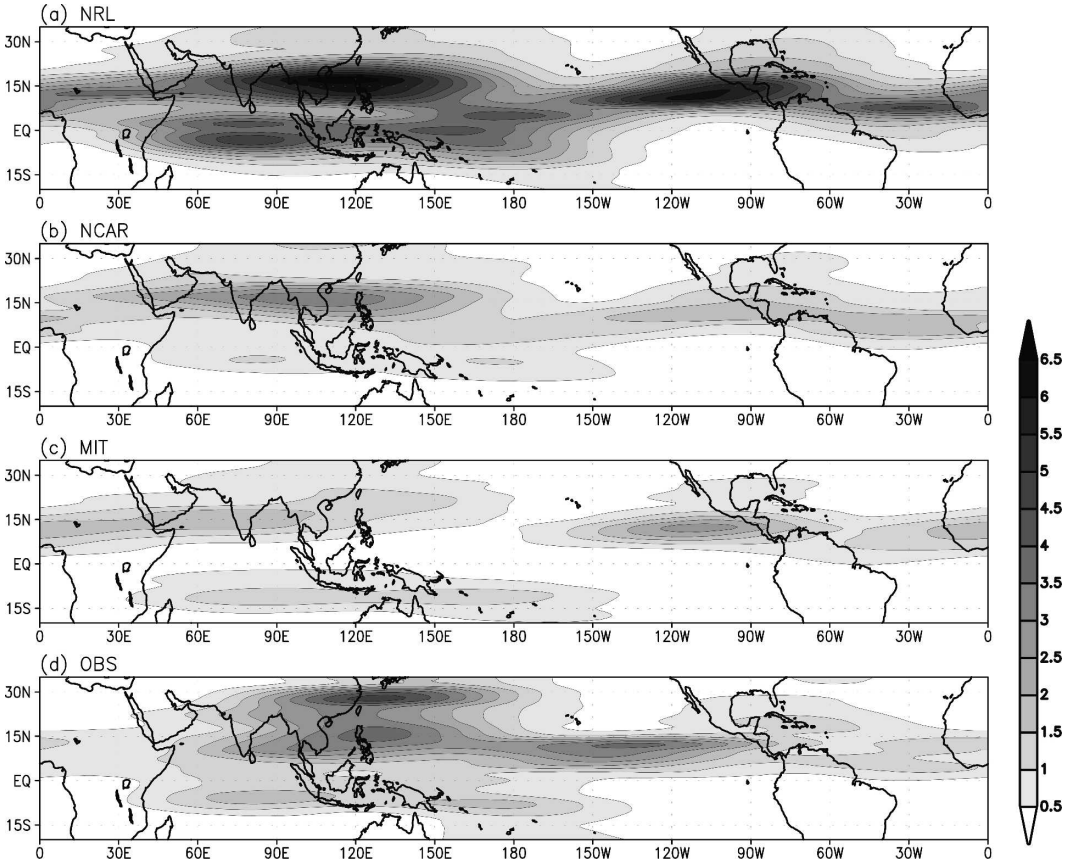

FIG. 10. Geographical distribution of variance ($mm^2\ day^{-2}$) of the wavenumber–frequency filtered precipitation for different convective schemes compared with a similar plot calculated from observations. Filtering is carried out in the wavenumber domain −2 to −5 and period range 25–80 days.

wami (2004). The meridional structure of the lower frequency wave can be considered as an $n = 2$ equatorial Rossby wave translated to north of the equator by about 12° by the mean wind. However, the meridional structure could also be obtained by an appropriate superposition of $n = 1$, 2, and 3 modes. Therefore, a definitive characterization of the Rossby mode is not possible at this time. Possibility of such Rossby waves playing a role in producing breaks in the monsoon was indicated by Krishnan et al. (2000).

6. Relationship between the simulated seasonal mean and the ISOs

It was noted earlier that the NCAR and MIT schemes fail to simulate the northward propagation of the ISO anomalies across the equator from about 5°S to about 10°N over the Indian monsoon region. The two models also have poor simulation of the eastward propagating component of the summer ISO. How does the systematic bias in the simulation of the summer ISOs related to systematic bias in simulation of the model's climatology? The northward propagation over the Indian monsoon region is examined first followed by examination of the relative contribution of eastward and westward propagating modes. Jiang et al. (2004) proposed two internal dynamics mechanisms to understand the cause of northward propagation of monsoon ISOs. According to the first, an easterly vertical shear of mean zonal winds causes generation of barotropic cyclonic vorticity, 2.5° north of the heating maximum due to coupling between free-atmosphere baroclinic and barotropic modes. The induced barotropic vorticity causes a maximum moisture convergence in the planetary boundary layer (PBL) north of the heating maximum leading to a northward shift of convective heating. This mechanism is effective away from the equator in the Northern Hemisphere. The second mechanism involves anomalous moisture convergence north of the heating by anomalous winds in the presence of a positive gradient of the mean meridional specific humidity. We have examined the reason for lack of northward

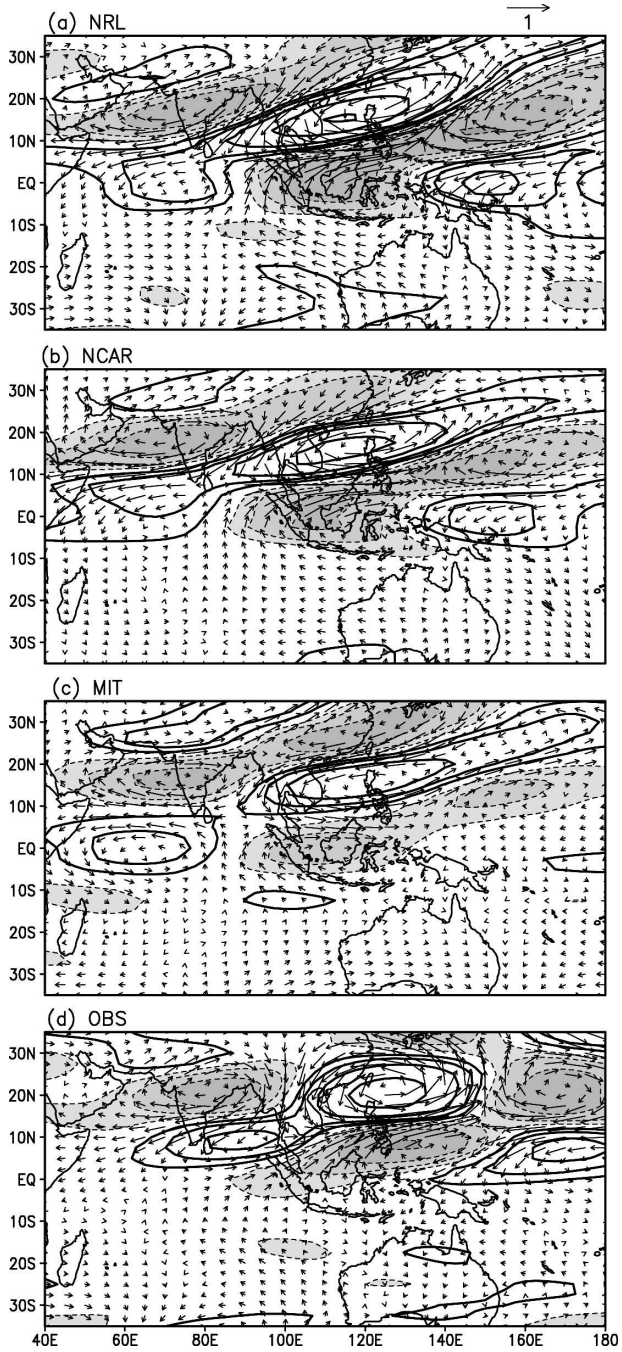

FIG. 11. Zero-lag structure of the westward propagating component of wavenumber–frequency filtered 850-hPa winds (m s^{-1}) and relative vorticity (10^{-6} s^{-1}) for different convective schemes compared with a similar plot calculated from the reanalysis dataset.

propagation in model simulations of the NCAR and MIT schemes in intraseasonal time scales in the context of this theory. Figure. 12a shows the mean specific humidity profile calculated from FSUGSM simulations with three different convection schemes averaged over 70°–100°E and plotted as a function of latitude and is compared with a similar profile calculated from the NCEP–NCAR reanalysis product. When compared to the observed specific humidity profile, the MIT and NCAR schemes show a negative meridional gradient in the mean specific humidity profile around the equator (10°S–10°N), which may be the reason for the poor simulation of northward propagation characteristics (see Figs. 8b,c). The NRL scheme shows a weak positive gradient in the specific humidity profile in the equatorial region. Although the magnitude of mean humidity is systematically lower than the observed of the NRL scheme, the correct meridional gradient appears to be responsible for better northward propagation of the simulated ISOs (see Fig. 8a). Figure 12b shows vertical zonal wind shear ($U_{850} - U_{200}$) calculated from model simulations averaged over the domain 40°–100°E and plotted as a function of latitude. A similar profile constructed from NCEP–NCAR reanalysis is also shown. It may be noted that for all three convective schemes, the vertical shear is significantly weaker than for NCEP between 10°S and 10°N. Thus, the vertical wind shear does not seem to play a crucial role in northward propagation close to the equator (Jiang et al. 2004). The MIT scheme simulates zonal wind shear greater than 20 m s^{-1} extending beyond 20°N. This is consistent with northward propagation in the MIT scheme (Fig. 8c) extending from about 10°N to about 25°N. Thus, the poor northward propagation in all schemes between 10°S to 10°N is believed to be related mainly to the poor simulation of the meridional gradient of mean humidity. However, the mean humidity distribution is closely related to the mean precipitation distribution. Poor northward propagation of ISOs simulated by the NCAR and MIT schemes is, therefore, indirectly related to biases in simulating mean precipitation distribution.

Comparing the three convective schemes employed in the FSUGSM, the NRL scheme seems to simulate the propagation characteristics of monsoon ISOs better. This may be due to the better simulation of seasonal mean precipitation by this scheme (see Fig. 3). Since the ISOs are convective instability that grows on the background mean flow, it may be concluded that better simulation of space–time characteristics of monsoon ISOs in the NRL scheme is related to better simulation of the background mean. At this point, we note that the pattern correlation between simulated seasonal mean precipitation by the MIT scheme with the observed seasonal mean precipitation over the Indian monsoon region is actually better than that of the NRL scheme. Thus, better simulation of the seasonal mean over a small region (such as Indian monsoon region) is

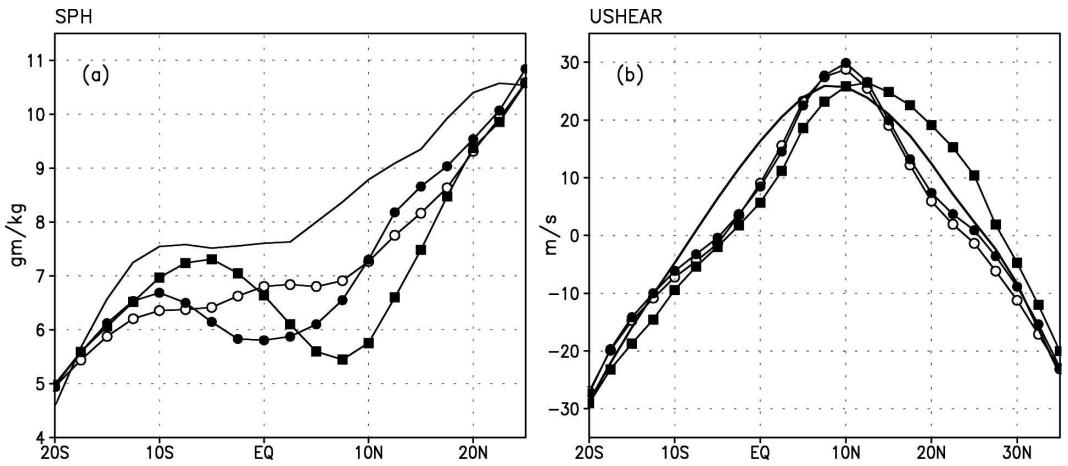

FIG. 12. Mean specific humidity gradient and zonal wind shear. (a) JJAS mean specific humidity (g kg^{-1}) averaged over 70°–100°E is plotted against latitude. (b) JJAS mean zonal wind shear (m s^{-1}) averaged over 40°–100°E is plotted against latitude. Zonal wind shear is calculated as $U_{850} - U_{200}$. Profiles with open circle represent the NRL scheme, closed circle represents NCAR scheme, closed square represents the MIT scheme, while the solid line represents observations.

not sufficient for better simulation of summer monsoon ISOs. Better simulation of the seasonal mean monsoon, at least over the entire Indo–west Pacific domain, is required for the better simulation of monsoon ISOs. This point is illustrated in Fig. 13a, where we plot the spatial correlation between model simulated seasonal mean precipitation and observed precipitation in the Indo–west Pacific domain (as listed in Table 2) versus the ratio between averaged power in the wavenumber–frequency spectral domain in the intraseasonal time scales for the eastward propagating component and that for the westward propagating component. Averaged power is defined as the spectral power averaged between 25 and 80 days and (+)2 to (+)5 wavenumbers for the eastward propagating mode and (−)2 to (−)5 wavenumbers for the the westward propagating mode. The ratio for observed precipitation is also plotted for comparison. A near-linear plot indicates that the scheme with higher spatial correlation simulates better eastward propagation relative to westward propagation. Schemes like MIT, whose simulation of seasonal mean in the Indo–west Pacific domain is poor, simulates stronger westward propagation than eastward propagation. A similar plot of 850-hPa zonal winds also shows a linear plot between spatial correlation versus averaged power (Fig. 13b).

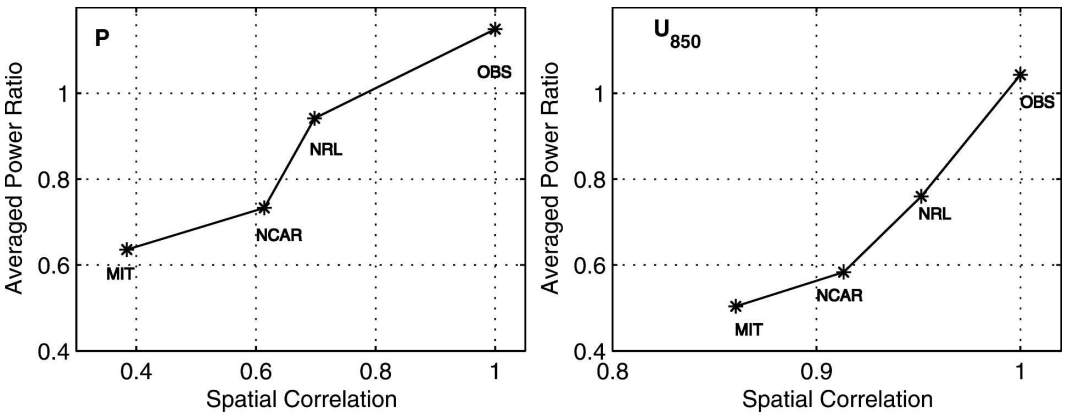

FIG. 13. Relationship with the simulation of seasonal mean and the ISOs: (a) spatial correlation between model simulated seasonal mean precipitation and observed precipitation in the Indo–west Pacific domain (as listed in Table 2) vs ratio between averaged power in the wavenumber–frequency spectral domain in the intraseasonal time scales for the eastward propagating component and that for the westward propagating component; (b) as in (a) but for 850-hPa zonal winds.

We recognize that results presented in Fig. 13 are based on rather small sample and need to be verified with more cumulus schemes and more models. However, they are quite instructive and indicate that models with significant bias in simulating pattern of seasonal mean precipitation even over the tropical Pacific domain would simulate unrealistic monsoon ISOs. When examining relationship between seasonal mean and ISO simulation by models, different gross measures of the background mean such as amplitude of seasonal cycle averaged over the tropical belt (Slingo et al. 1996) or zonal variation of latitudinally averaged seasonal mean (Lin et al. 2006) have been used in earlier studies. Here, we propose a different measure, namely, that the spatial pattern of the background mean over the tropical Indo–Pacific is important for simulating the propagation characteristics of the summer ISOs. This possibility occurred to us from the observation that the spatial structure of the dominant ISO mode has a large projection on the season mean structure.

7. Summary and discussion

Using simulations from the upgraded version of the FSUGSM with three different convective parameterization schemes, major characteristics of South Asian summer intraseasonal oscillations are studied and validated with observed datasets. In addition to assessing the simulation of mean summer monsoon rainfall and monsoon intraseasonal variability, propagation characteristics of simulated monsoon ISOs are investigated in detail. Probable reasons for the systematic error seen in simulating monsoon ISOs are identified. Nature of the westward propagating mode seen in model simulations as well as in observations is investigated. Analysis and discussions are also presented to address the question on whether the simulation of seasonal mean determines the characteristics of monsoon ISOs.

Three different convection schemes, NRL (Arakawa–Schubert), NCAR (Zhang and McFarlane), and MIT (Emanuel), were used in the FSUGSM to generate an ensemble of model simulations to study monsoon intraseasonal oscillations. The northern summer (JJAS) seasonal mean simulated by the three schemes are distinctly different from each other. The NRL and NCAR schemes seem to exhibit better simulation of the seasonal mean precipitation compared to observations, although the simulated magnitudes are higher. Though, the MIT scheme shows good simulation of seasonal mean precipitation over the Indian continent and Bay of Bengal, it exhibits poor simulation of precipitation over the western Pacific and Maritime Continent. Simulation of a secondary zone of precipitation over the warm waters of the Indian Ocean is problematic in all schemes. While the NRL and NCAR schemes simulate peak rainfall to west of the observed location, the MIT scheme simulates it southward of the observed location. Comparison of simulated intraseasonal oscillations by different cumulus schemes with observations indicates systematic errors in simulating the ISOs that seem to be related to the systematic bias in simulating the seasonal mean. Among the three cumulus schemes, NRL seems to show better simulation of both seasonal mean monsoon precipitation and intraseasonal variance.

A major character of monsoon ISOs is the northward and eastward propagation of precipitation anomalies from south equatorial Indian Ocean to about 25°N. While the NRL scheme shows reasonable simulation of northward propagation of filtered anomalies, it is limited to north of 10°N in both NCAR and MIT schemes. Reasons for the difference in the northward propagation of rainfall anomalies were identified within the context of the theory suggested by Jiang et al. (2004). The simulated easterly vertical shear of zonal wind between 10°S and 10°N are similar in all three schemes. Therefore, it appears that the incorrect simulation of the gradient of mean humidity over the equatorial Indian Ocean is responsible for the lack of northward propagation seen in the NCAR and MIT schemes over the equatorial Indian Ocean. The climatological humidity distribution being closely related to climatological precipitation, inability of the NCAR and MIT schemes to simulate the observed northward propagation of the dominant ISO is related to the bias in simulating the meridional structure of the mean precipitation.

Regarding eastward propagation of precipitation anomalies, the ratio between amplitude of the eastward propagating 25–80-day ISO mode and that of the westward propagating one in observation is slightly larger than unity, resulting in dominance of the eastward propagating component. In the NRL simulation it is close to unity, while it is much smaller in the NCAR and MIT schemes. Though the MIT scheme has better simulation of seasonal mean precipitation and intraseasonal variance over the Indian subcontinent and Bay of Bengal, it shows poor simulation of propagation characteristics. This shows that realistic simulation of the entire Indo–Pacific domain is important for better simulation of propagation characteristics and intraseasonal variance. As the westward propagating ISO mode plays an important role in the model's ability to simulate the observed ISO characteristics, the nature of westward propagation seen in the model simulations is investigated in detail. It is found that the westward propagating mode seen in model simulation is a Rossby

wave with period between 25 and 80 days and wavelength of about 10 000 km. It appears to be an equatorial Rossby wave modified by the background mean shear.

Although based on a limited sample, an important message that emerges from our study is that the scheme which simulates better seasonal mean pattern of rainfall over the Indo–Pacific domain better simulates the eastward propagating mode relative to the westward propagating one and, hence, better simulation of northeastward propagation of monsoon ISOs. An important question follows: What makes the NRL scheme simulate the spatial pattern of mean rainfall and ISO characteristics more realistically compared to the NCAR and MIT schemes? A related question is whether a better simulation of the seasonal mean pattern leads to a better simulation of the ISO or a better simulation of the ISO by a cumulus scheme eventually leads to a better seasonal mean pattern. These are difficult questions and an unambiguous answer is outside the scope of the present study. Here we provide some qualitative arguments to speculate on one possibility. As the spatial pattern of the dominant ISO mode has a strong projection on the seasonal mean, the statistical average of the ISOs during the summer season contributes to the seasonal mean (Sperber et al. 2000; Goswami and Ajayamohan 2001) and its interannual variability. Also ISOs are essentially convectively coupled instability. Thus, the cumulus parameterization schemes determine the nature of the simulated ISOs first, which in turn determine the seasonal mean structure. Hence the summer monsoon ISOs may be considered as the primary building block of the south Asian monsoon. Thus, systematic biases of the simulated seasonal mean could be related to the systematic bias of the simulated ISOs. We believe that this relationship is at the heart of the link between the simulated seasonal mean and ISO space–time characteristics shown here. The original question then reduces to answering why the NRL scheme simulates the ISOs realistically while the others could not. More basic research will be required to answer this question.

Since, the ISOs are linked to interannual variability of the seasonal mean, successful prediction of the seasonal mean requires a model with better simulation of space–time characteristics of the monsoon ISOs. Our exercise reveals that for better prediction of the seasonal mean, the model climatology must have minimum bias over the entire Indo–Pacific basin and not only over the Indian monsoon region.

Acknowledgments. Model simulations were carried out when one of the authors, R. S. Ajayamohan was a visiting scientist at Center for Ocean–Atmospheric Prediction Studies (COAPS), Florida State University. R. S. Ajayamohan would like to thank Prof. James J. O'Brien, who gave an opportunity to work at COAPS. Thanks are due to Drs. D. W. Shin, Steve Cocke, and T. E. LaRow for helpful discussions for carrying out the model simulations. Thanks to Matthew Wheeler for providing codes to calculate wavenumber–frequency spectra. We acknowledge Jaison Kurian, CAOS, IISc for helping us perform some calculations using wavenumber–frequency spectra. We thank two anonymous reviewers for their valuable comments that helped improve the manuscript. We are thankful to Department of Ocean Development, India, for a grant.

REFERENCES

Ajayamohan, R. S., and B. N. Goswami, 2003: Potential predictability of the Asian summer monsoon on monthly and seasonal time scales. *Meteor. Atmos. Phys.,* **84,** 83–100.

Annamalai, H., and J. M. Slingo, 2001: Active/break cycles: Diagnosis of the intraseasonal variability of the Asian summer monsoon. *Climate Dyn.,* **18,** 85–102.

Businger, J. A., J. C. Wyngaard, Y. Izumi, and E. F. Bradly, 1971: Flux profile relationship in the atmospheric surface layer. *J. Atmos. Sci.,* **28,** 181–189.

Chatterjee, P., and B. N. Goswami, 2004: Structure, genesis and scale selection of the tropical quasi-biweekly mode. *Quart. J. Roy. Meteor. Soc.,* **130,** 1171–1194.

Cocke, S., 1998: Case study of ERIN using the FSU nested regional spectral model. *Mon. Wea. Rev.,* **126,** 1337–1346.

——, and T. E. LaRow, 2000: Seasonal predictions using a regional spectral model embedded within a coupled ocean–atmospheric model. *Mon. Wea. Rev.,* **128,** 689–708.

Duchon, C. E., 1979: Lanczos filtering on one and two dimensions. *J. Appl. Meteor.,* **18,** 1016–1022.

Emanuel, K. A., 1991: A scheme for representing cumulus convection in large-scale models. *J. Atmos. Sci.,* **48,** 2313–2335.

——, and M. Zivkovic-Rothman, 1999: Development and evaluation of a convective scheme for use in climate models. *J. Atmos. Sci.,* **56,** 1766–1782.

Fu, X., B. Wang, and T. Li, 2002: Impacts of air–sea coupling on the simulation of mean Asian summer monsoon in ECHAM4 model. *Mon. Wea. Rev.,* **130,** 2889–2904.

——, ——, ——, and J. McCreary, 2003: Coupling between northward propagating, intraseasonal oscillations and sea surface temperature in the Indian Ocean. *J. Atmos. Sci.,* **60,** 1733–1753.

Gadgil, S., 2003: The Indian monsoon and its variability. *Annu. Rev. Earth Planet. Sci.,* **31,** 429–467.

——, and S. Sajani, 1998: Monsoon precipitation in the AMIP runs. *Climate Dyn.,* **14,** 659–689.

Goswami, B. N., 2005: South Asian monsoon. *Intraseasonal Variability in the Atmosphere–Ocean Climate System,* W. K. M. Lau and D. E. Waliser, Eds., Praxis Springer, 19–61.

——, and R. S. Ajayamohan, 2001: Intraseasonal oscillations and interannual variability of the Indian summer monsoon. *J. Climate,* **14,** 1180–1198.

——, ——, P. K. Xavier, and D. Sengupta, 2003: Clustering of synoptic activity by Indian summer monsoon intraseasonal

oscillations. *Geophys. Res. Lett.,* **30,** 1431, doi:10.1029/2002GL016734.

Harshvardhan, and T. G. Corsetti, 1984: Longwave parameterization of the UCLA/GLAS GCM. Tech. Memo. 86072, Goddard Space Flight Center, 51 pp.

Hogan, T. F., and T. E. Rosmond, 1991: The description of the Navy Operational Global Atmospheric Prediction System's spectral forecast model. *Mon. Wea. Rev.,* **119,** 1786–1815.

Huffman, G. J., R. F. Adler, M. M. Morrissey, S. Curtis, R. Joyce, B. McGavock, and J. Sisskind, 2001: Global precipitation at one degree daily resolution from multisatellite observations. *J. Hydrometeor.,* **2,** 35–50.

Jiang, X., T. Li, and B. Wang, 2004: Structures and mechanisms of the northward-propagating boreal summer intraseasonal oscillation. *J. Climate,* **17,** 1022–1039.

Kalnay, E., and Coauthors, 1996: The NCEP/NCAR 40-Year Reanalysis project. *Bull. Amer. Meteor. Soc.,* **77,** 437–471.

Kanamitsu, N., 1975: On numerical prediction over a tropical belt. Tech. Rep. 75-1, Dept. of Meteorology, The Florida State University, 282 pp.

——, K. Tada, K. Kudo, T. Sata, and N. Isa, 1983: Description of JMA operational spectral model. *J. Meteor. Soc. Japan,* **61,** 812–828.

Krishnamurti, T. N., and H. N. Bhalme, 1976: Oscillations of monsoon system. Part I: Observational aspects. *J. Atmos. Sci.,* **33,** 1937–1954.

——, S. Low-Nam, and R. Pasch, 1983: Cumulus parameterization and rainfall rates II. *Mon. Wea. Rev.,* **111,** 815–828.

——, J. Xue, H. S. Bedi, K. Ingles, and D. Oosterhof, 1991: Physical initialization for numerical weather prediction over the tropics. *Tellus,* **43A/B,** 53–81.

Krishnan, R., C. Zhang, and M. Sugi, 2000: Dynamics of breaks in the Indian summer monsoon. *J. Atmos. Sci.,* **57,** 1354–1372.

Lacis, A. A., and J. E. Hansen, 1974: A parameterization for the absorption of solar radiation in the earth's atmosphere. *J. Atmos. Sci.,* **31,** 118–133.

LaRow, T. E., and T. N. Krishnamurti, 1998: ENSO prediction using an ocean–atmosphere model. *Tellus,* **50A,** 76–94.

Lin, J.-L., and Coauthors, 2006: Tropical intraseasonal variability in 14 IPCC AR4 climate models. Part I: Convective signals. *J. Climate,* **19,** 2665–2690.

Louis, J. F., 1981: A parametric model of vertical eddy fluxes in the atmosphere. *Bound.-Layer Meteor.,* **17,** 187–202.

Maloney, E. D., and D. L. Hartmann, 2001: The sensitivity of intraseasonal variability in the NCAR CCM3 to changes in convective parameterization. *J. Climate,* **14,** 2015–2034.

Ramage, C. S., 1971: *Monsoon Meteorology.* International Geophysics Series, Vol. 15, Academic Press, 296 pp.

Reynolds, R. W., and T. M. Smith, 1994: Improved global sea surface temperature analyses using optimum interpolation. *J. Climate,* **7,** 929–948.

Rosmond, T. E., 1992: The design and testing of the Navy Operational Global Atmospheric Prediction System. *Wea. Forecasting,* **7,** 262–272.

Sengupta, D., R. Senan, and B. N. Goswami, 2001: Origin of intraseasonal variability of circulation in the tropical central Indian Ocean. *Geophys. Res. Lett.,* **28,** 1267–1270.

Shukla, J., 1987: Interannual variability of monsoon. *Monsoons,* J. S. Fein and P. L. Stephens, Eds., Wiley and Sons, 399–464.

Sikka, D. R., and S. Gadgil, 1980: On the maximum cloud zone and the ITCZ over Indian longitude during southwest monsoon. *Mon. Wea. Rev.,* **108,** 1840–1853.

Slingo, J. M., and Coauthors, 1996: Intraseasonal oscillation in 15 atmospheric general circulation models: Results from an AMIP diagnostic subproject. *Climate Dyn.,* **12,** 325–357.

Sperber, K. R., J. M. Slingo, and H. Annamalai, 2000: Predictability and the relationship between subseasonal and interannual variability during the Asian summer monsoons. *Quart. J. Roy. Meteor. Soc.,* **126,** 2545–2574.

Tiedke, M., 1984: The sensitivity of the time mean large-scale flow to cumulus convection in the ECMWF model. *Proc. Workshop on Convection in Large-Scale Numerical Models,* Reading, United Kingdom, ECMWF, 297–317.

Waliser, D., and Coauthors, 2003: AGCM simulations of intraseasonal variability associated with the Asian summer monsoon. *Climate Dyn.,* **21,** 423–446.

Wang, B., and X. Xie, 1996: Low-frequency equatorial waves in vertically sheared zonal flow. Part I: Stable waves. *J. Atmos. Sci.,* **53,** 449–467.

Webster, P. J., V. O. Magana, T. N. Palmer, J. Shuka, R. T. Tomas, M. Yanai, and T. Yasunari, 1998: Monsoons: Processes, predictability, and the prospects of prediction. *J. Geophys. Res.,* **103** (C7), 14 451–14 510.

Wheeler, M., and G. N. Kiladis, 1999: Convectively coupled equatorial waves: Analysis of clouds and temperature in the wavenumber–frequency domain. *J. Atmos. Sci.,* **56,** 374–399.

——, ——, and P. J. Webster, 2000: Large-scale dynamical fields associated with convectively coupled equatorial waves. *J. Atmos. Sci.,* **57,** 613–640.

Xie, P., and P. A. Arkin, 1997: Global precipitation: A 17-year monthly analysis based on gauge observations, satellite estimates and numerical model outputs. *Bull. Amer. Meteor. Soc.,* **78,** 2539–2558.

Xie, X., and B. Wang, 1996: Low-frequency equatorial waves in vertically sheared zonal flow. Part II: Unstable waves. *J. Atmos. Sci.,* **53,** 3589–3605.

Yasunari, T., 1979: Cloudiness fluctuation associated with the Northern Hemisphere summer monsoon. *J. Meteor. Soc. Japan,* **57,** 227–242.

Zhang, G. J., and N. A. McFarlane, 1995: Sensitivity of climate simulations to the parameterizations of cumulus convection in the Canadian Climate Centre general circulation model. *Atmos.–Ocean,* **33,** 407–446.